Monte Carlo simulations were used as estimates of the true fractional success rates and the correlation coefficient $\rho_{ij}$ was taken as unity (its maximum value) for all $i$ and $j$. With the assumption of a normal distribution of the error, approximate 95% confidence limits are given by $K \pm 2\sigma_K$. In all of our calculations errors associated with numerical integration were negligible in comparison with the statistical errors.

Unfortunately, estimation of the errors in partition coefficients when there are attractive interactions is more difficult. The determination of $p(\beta)$ no longer follows binomial statistics because there are now $n + 2$ possible "states" a chain can occupy (failure or success with zero to $n$ mass points in the interaction region) as compared with two "states" (failure or success) in the purely steric partitioning case. In addition, the exponential weightings employed in the calculation of $p(\beta)$ tend to exaggerate statistical fluctuations, especially at large $n$ and high interaction energies where peaks appeared in the $p(\beta)$ profiles. Recognizing this, we estimated the additional error in the partition coefficient due to the introduction of the interaction energy as the difference between an approximate maximum partition coefficient and the partition coefficient calculated by the usual procedure. The maximum partition coefficient was estimated by performing the integration using the trapezoidal rule between local maxima in the $p(\beta)$ profiles (including a correction for the larger integration step size). This additional error was added to the error estimate for the purely steric partition coefficient to obtain the overall error in partition coefficients when attractive interactions are present.

## References and Notes


(1) Casassa, E. F. *J. Polym. Sci., Part B* **1967**, *5*, 773.
(2) Casassa, E. F.; Tagami, Y. *Macromolecules* **1969**, *2*, 14.
(3) Daoud, M.; de Gennes, P.-G. *J. Phys. (Les Ulis, Fr.)* **1977**, *38*, 85.
(4) Giddings, J. C.; Kucera, E.; Russell, C. P.; Myers, M. N. *J. Phys. Chem.* **1968**, *72*, 4397.
(5) Priest, R. G. *J. Appl. Phys.* **1981**, *52*, 5930.
(6) Kramers, H. A. *J. Chem. Phys.* **1946**, *14*, 415.
(7) Scheutjens, J. M.; Fleer, G. J. *Macromolecules* **1985**, *18*, 1882.
(8) DiMarzio, E. A.; Rubin, R. J. *J. Chem. Phys.* **1971**, *55*, 4318.
(9) Zhulina, E. B.; Gorbunov, A. A.; Birshtein, T. M.; Skvortsov, A. M. *Biopolymers* **1982**, *21*, 1021.
(10) Gorbunov, A. A.; Zhulina, E. B.; Skvortsov, A. M. *Polymer* **1982**, *23*, 1133.
(11) Fluendy, M. In *Markov Chains and Monte Carlo Calculations in Polymer Science*; Lowry, G. G., Ed.; Marcel Dekker: New York, 1970; pp 45-90.
(12) Casassa, E. F. *J. Polym. Sci., Part A-2* **1972**, *10*, 381.
(13) Box, G. E. P.; Hunter, W. G.; Hunter, J. S. *Statistics for Experimenters*; Wiley: New York, 1978; pp 57-92.
(14) Aubert, J. H.; Tirrell, M. *J. Chem. Phys.* **1982**, *77*, 553.


# Confined Star Polymers


**A. Halperin***

*The Fritz Haber Research Center for Molecular Dynamics, The Hebrew University of Jerusalem, Jerusalem 91904, Israel*

**S. Alexander**

*The Racah Institute of Physics, The Hebrew University of Jerusalem, Jerusalem 91904, Israel.*

*Received August 11, 1986*


ABSTRACT: The behavior of star polymers confined to a narrow slit in a good solvent is investigated by using scaling ("blob") analysis. In the confined star we distinguish (1) an interior region with spherical symmetry in which the confinement has no effect, (2) an intermediate region where the global spherical symmetry is lost, but the blob structure is still three-dimensional, and (3) an exterior region characterized by cylindrical symmetry. The concentration profile and the radius of the isolated star are obtained as well as its confinement free energy. Concentration effects are discussed. For this system we find six regimes rather than the five found for confined linear chains.


## I. Introduction

The interest in polymer confinement is twofold: On the applied side, it is relevant to the study of polymer solution in porous media,[1] wetting by such solutions,[2] etc. From a theoretical point of view, the emphasis is on the various crossovers between three- and two-(one) dimensional behavior, which are associated with confined polymers. Most research efforts in this area have been directed toward the understanding of *linear* macromolecules under confinement.[3] In the following we will consider the theory of confined *star* polymers.

In recent years there has been an increased interest in branched polymers.[4] Of the various kinds of branched polymers, star-branched polymers may be synthesized so as to obtain well-characterized stars at varying numbers of arms (functionality). It is thus possible to probe their configurational properties as a function of their molecular weight and functionality. Such investigations were carried out on dilute star polymer solutions using static and dynamic light scattering as well as intrinsic viscosity measurements.[5]

Early theoretical studies of star polymers assumed Gaussian statistics. Their predictions, however, were not in good agreement with experimental results on stars with high functionalities. A scaling theory developed by Daoud and Cotton[5-7] generally accounts for the experimental results in this regime. Nevertheless, both experiment and a renormalization group study of Miyake and Freed[8] suggest that the Daoud–Cotton (DC) model is only valid for high functionalities (>7). On the other hand, for high functionalities, one may worry about spurious effects due to the complicated structure of the center. It is possible to avoid this difficulty if we replace the star polymers by colloidal particles stabilized by grafted linear polymers.[6,10] Bearing these considerations in mind, we will base our discussion on the DC model. We will consider a solution of star polymers, in good solvent, confined to a slit, i.e., between parallel plates. The slit walls will be assumed to

0024-9297/87/2220-1146$01.50/0 

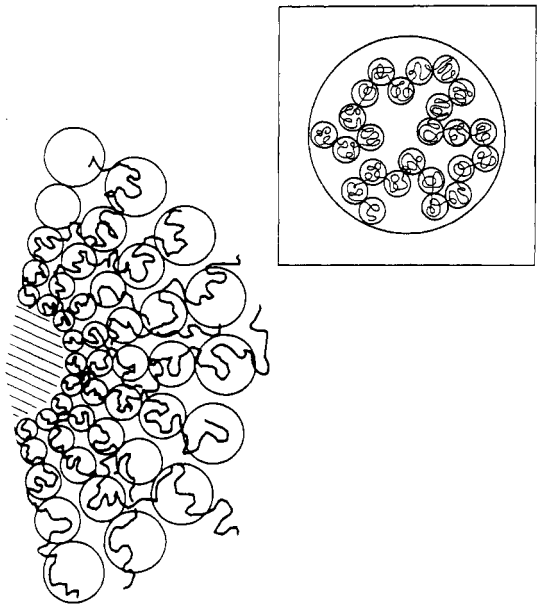

**Figure 1.** Daoud–Cotton conception of a star polymer. The figure shows a partial cross section of a free star. The hatched region denotes the core. In both the ideal and swollen regions, the blobs are arranged in spherical shells of thickness $\xi(r)$. In each shell, there are $f$ blobs. The inset shows a two-dimensional "superblob" of the type found in the exterior region of the confined star. The superblob is composed of three-dimensional blobs of size $D$.

be nonadsorbing. Our results, with obvious adaptations, apply to solutions of colloidal particles stabilized by grafted linear chains.

## II. Daoud–Cotton Model for Star-Branched Polymers

In the following we will summarize the DC analysis of free nonconfined stars. Consider a star-branched polymer mode of $f$ identical arms joined at the center. Each branch consists of $N$ monomers of size $a$. The DC model[5] is based on two observations: (1) star polymers have spherical symmetry; (2) one expects the monomer volume fraction, $\phi$, to be a decreasing function of the distance from the center of the star, $r$. To obtain an explicit form for $\phi(r)$ DC analyze the configuration of the star in terms of "blobs", i.e., chain segments characterized by single linear chain behavior. Blobs occupy regions of size $\xi$, which depend on the local monomer concentration. The blob picture, as used to obtain the configuration of a *single* star, is related to the "temperature blob" model.[9] DC postulate the following: (1) $\xi$ depends on $r$ only: $\xi = \xi(r)$. This means that the concentration profile is *self-similar* and thus $\xi \sim r$. (2) In a spherical shell of radius $r$ and thickness $\xi(r)$ there are $f$ blobs (Figure 1). The second postulate determines the $f$ dependence of $\xi$: the volume of a spherical shell $r^2\xi$ is equal to that of $f$ blobs of volume $\xi^3$ each; thus

$$\xi \sim r/f^{1/2} \tag{II.1}$$

DC then argue that one may expect to find three zones in the star: (1) a core in which the monomers are closed packed, $\phi \sim 1$; (2) an ideal or Gaussian zone, where $\xi$ is small enough so that the blobs are ideal,[9] i.e.

$$\xi(r) \sim n^{1/2}(r)a \tag{II.2}$$

where $n(r) = n(\xi(r))$ is the number of monomers in a blob of size $\xi$; and (3) an exterior "corona", where $\xi$ is higher still and where excluded volume interactions are important within the blobs, i.e.

$$\xi(r) \sim n^{3/5}(r)v^{1/5}a \tag{II.3}$$

where $v = {}^1/_2 - \chi$ and $\chi$ is the Flory interaction parameter. On comparing eq II.1 to II.3 we obtain an explicit form for $n(r)$, which in turn enables us to calculate $\phi(r)$ using

$$\phi(r) \sim \frac{fn(r)a^3}{r^2\xi(r)} \tag{II.4}$$

The crossover distances between different zones are obtained by matching the $\phi$ value of neighboring regions. This leads to the following picture of the free isolated star: (1) a core zone where

$$\phi \sim 1 \qquad 0 < r < r_c \sim f^{1/2}a \tag{II.5}$$

(2) an ideal zone where

$$\phi \sim f^{1/2}(a/r) \qquad r_c < r < r_i \sim f^{1/2}v^{-1}a \tag{II.6}$$

and (3) a swollen zone where

$$\phi \sim f^{2/3}(a/r)^{4/3}v^{-1/3} \qquad r_i < r < R \tag{II.7}$$

where $R$ is the radius of the star. To obtain $R$ we use the condition

$$Nfa^3 = \int_0^R \phi(r)\, \mathbf{dr} \tag{II.8}$$

We find

$$R \sim f^{1/5}N^{3/5}v^{1/5}a \qquad N \gg f^{1/2}v^{-2} \tag{II.9a}$$

$$R \sim f^{1/4}N^{1/2}a \qquad f^{1/2}v^{-2} \gg N \gg f^{1/2} \tag{II.9b}$$

Once we know $R$ we may consider concentration effects. We first obtain $C^*$ for star polymers

$$C^* \sim f^{2/5}N^{-4/5}v^{-3/5}a^{-3} \qquad N \gg f^{1/2}v^{-2}$$

$$C^* \sim f^{1/2}N^{-1/2}a^{-3} \qquad f^{1/2}v^{-2} \gg N \gg f^{1/2} \tag{II.10}$$

Once we increase the concentration past $C^*$, arms of different stars entangle and locally resemble a semidilute solution of linear polymers with a constant concentration $C$. As a result, a new crossover distance $\chi(C)$ appears in the problem, given by

$$\chi(C) \sim f^{1/2}(Ca^3)^{-3/4}v^{-1/4}a \tag{II.11}$$

$\chi(C)$ is defined by the equality of $\phi(\chi)$ in the star and the "bulk" monomer volume fraction $ca^3$. For $r < \chi(C)$ we find a single-star behavior, while for $r > \chi(C)$ concentration effects dominate; i.e., we find "concentration blobs" of single size

$$\xi(C) \sim (Ca^3)^{-3/4}v^{1/4}a \tag{II.12}$$

In this regime the star radius is smaller than that of an isolated star. It is given by

$$R \sim \chi(C) + \Delta \tag{II.13}$$

The bulk concentration $C$ determines $\chi(C)$ and thus (through eq II.9) the number of monomers $n_a$ of each arm in the single-star zone ($r < \chi(C)$). The remaining $N - n_a$ monomers are grouped into $N_c$ concentration blobs. The concentration blobs behave as an ideal chain with links of size $\xi(C)$. We thus obtain

$$\Delta \sim n_c^{1/2}\xi(C) \sim (N - f^{1/2}(Ca^3)^{-5/4}v^{-3/4})^{1/2}(Ca^3)^{-1/8}v^{1/8}a \tag{II.14}$$

For concentrations below $f^{2/5}C^*$, $R \sim \chi$, while for much higher concentrations, we expect to find $R \sim N^{1/2} \times (Ca^3)^{-1/8}v^{1/8}a$.

## III. A Single Star in a Slit

Let us now place a dilute solution of polymers in an infinite slit of width $D$ such that $D$ is smaller than $R$. We will mostly consider the case $r_c \ll D \ll R$. For confined stars, as for free stars, we expect $\phi$ to be a decreasing function of $r$. We are thus led to postulate the same sequence of zones in the two cases. However, for confined stars this picutre is not complete because it fails to allow for the onset of two-dimensional behavior in the exterior regions of the star. It is thus necessary to refine the free-star structure by further subdivision. We distinguish between three regions according to the relative magnitudes of $R$, $\xi$, and $D$: (1) An interior region for which $R < D$ and $\xi < D$. This region retains the three-dimensional free-star structure. In particular, it has a spherical symmetry and a self-similar concentration profile with $\xi \sim r$. (2) An intermediate region where $R > D$ but $\xi < D$. Here, the global spherical symmetry is lost. We replace spherical shells of volume $r^2\xi$ by truncated spherical shells of volume $r\xi D$. The local blob structure is still three-dimensional; i.e., the blob volume is $\xi^3$. In this region $\xi$ is a function of both $r$ and $D$ and thus the concentration profile is *not* self-similar. (3) An exterior region where $R > D$ and $\xi > D$. This region is characterized by cylindrical rather than spherical symmetry, $\xi$ is again a function of $r$ alone, leading to a self-similar profile with $\xi \sim r$. Here, $\xi$ defines two-dimensional "superblobs" made of blobs of size $D$ set by the slit width. The blob volume is now given by $\xi^2 D$.

To quantify these observations we now follow DC and postulate that in any shell, spherical, truncated spherical, or cylindrical, there are $f$ blobs. To find $\xi(r)$ we equate the volume of a shell with that of $f$ blobs. In the intermediate region we have $f\xi^3 \sim r\xi D$ or

$$\xi \sim (rD/f)^{1/2} \tag{III.1}$$

In the exterior region we find $f\xi^2 D \sim r\xi D$, leading to

$$\xi \sim r/f \tag{III.2}$$

Note that in the intermediate region $\xi \sim r^{1/2}$ so that the concentration profile in this region is indeed not self-similar. While in the exterior region $\xi \sim r$ as in the interior region, the $f$ dependence in the two cases is different. In both regions the volume of a shell is given by $r\xi D$ rather than $r^2\xi$. As a result we must replace eq II.4 for $\phi$ by

$$\phi(r) \sim fn(r)a^3/(r\xi(r)D) \tag{III.3}$$

To proceed further we distinguish between two cases: (1) If $r_i \ll D \ll R$ the confinement affects the swollen zone only. The interior region includes the core, the ideal zone, and part of the swollen zone. The intermediate and exterior regions appear in the periphery of the swollen zone. Confined colloidal particles stabilized by grafted polymers fall under this heading, provided that the grafting density and the polymers' degree of polymerization are high enough. For this system $r_i$ stands for the radius of the colloidal particle. In this case there is no core or ideal zone. (2) When $r_c \ll D \ll r_i$ the confinement affects both the ideal and the swollen zones. The interior region includes the core and parts of the ideal zone. The intermediate region appears in the ideal zone followed by the exterior region, which includes the outer part of the ideal zone as well as all of the swollen zone.

Consider first the case $r_i \ll D \ll R$. Up to $r \sim D$ the free-star structure is not perturbed. To obtain $\phi(r)$ in the intermediate region we equate $\xi$ given by (III.1) to $\xi \sim n^{3/5}v^{1/5}a$. This leads to

$$n(r) \sim f^{-5/6}(r/a)^{5/6}(D/a)^{5/6}v^{-1/3} \tag{III.4}$$

Using eq III.1, III.3, and III.4, we find

$$\phi(r) \sim f^{2/3}(a/r)^{2/3}(a/D)^{2/3}v^{-1/3} \tag{III.5}$$

We now turn to the exterior region. Here the elementary unit is the "$D$ blob", defined by

$$D \sim g^{3/5}v^{1/5}a \tag{III.6}$$

where $g$ is the number of monomers in a $D$ blob. $n_b$ $D$ blobs are grouped into a superblob of size $\xi$ given by (III.2). Inside the superblobs the $D$ blobs obey two-dimensional self-avoiding random walk statistics (Figure 1)

$$\xi \sim n_b^{3/4}D \tag{III.7}$$

Upon comparing (III.7) and (III.2), we find

$$n_b \sim f^{-4/3}(r/D)^{4/3} \tag{III.8}$$

Combining (III.8) and (III.6), we obtain

$$n(r) = n_b g \sim f^{-4/3}(r/a)^{4/3}(D/a)^{1/3}v^{-1/3} \tag{III.9}$$

Substituting (III.9) and (III.2) in (III.3) yields

$$\phi(r) \sim f^{2/3}(a/r)^{2/3}(a/D)^{2/3}v^{-1/3} \tag{III.10}$$

Note that while $\phi(r)$ has the same form in the two regions, the two differ in the number of "elementary blobs" per shell. In the intermediate region there are $f$ blobs per shell while in the exterior region each shell contains $fn_b$ $D$ blobs. To complete the picture we must specify the crossover distances between the various regions. The crossover distance between the intermediate and the exterior regions, $r_{ie}$, is not obtainable by matching the $\phi(r)$ in the two regions (eq III.5 and III.10). As an alternative we use the condition $\xi \sim D$, obtaining

$$r_{ie} \sim fD \tag{III.11}$$

The crossover distance between the interior and the intermediate regions, $r_{ii}$, may be obtained by matching $\phi$ as given by eq III.5 and III.3, leading, as expected, to

$$r_{ii} \sim D \tag{III.12}$$

In the case $r_c \ll D \ll r_i$, the intermediate region is shifted into the ideal zone. To obtained $n(r)$ we equate (III.1) and $\xi \sim n^{1/2}(r)a$, obtaining

$$n(r) \sim f^{-1}(r/a)(D/a) \tag{III.13}$$

Using (III.1), (III.3), and (III.13), we find

$$\phi(r) \sim f^{1/2}(a/r)^{1/2}(a/D)^{1/2} \tag{III.14}$$

In this case we expect the exterior region to include part of the ideal zone as well as all of the swollen zone. To obtain $\phi$ in the ideal part of the exterior region, we equate (III.2) and $\xi \sim n^{1/2}(r)a$, leading to

$$n(r) \sim f^2(r/a)^2 \tag{III.15}$$

By using eq III.2, III.3, and III.15, we obtain

$$\phi \sim a/D \tag{III.16}$$

The form of $\phi(r)$ in the swollen zone of the exterior region is given by (III.10). By matching $\phi$ in the various regions, we find that $r_{ie}$ and $r_{ii}$, the boundaries of the intermediate region, are again given by (III.11) and (III.12), respectively. In this case, however, the crossover distance between the ideal and the swollen zones is modified by the confinement to $\tilde{r}_i$, given by

$$\tilde{r}_i \sim f(D/a)^{1/2}v^{-1/2}a \tag{III.17}$$

We have analyzed the conformation of an isolated star polymer under confinement in two cases. Our results are summarized in Table I. In both cases the three-zone

**Table I**

Case I: $r_i \ll D \ll R$

| $\phi(r)$ | $r$ | region | |
|---|---|---|---|
| 1 | $0 < r < r_c$ | core | interior region |
| $f^{1/2}(a/r)$ | $r_c < r < r_i$ | ideal, three-dimensional | |
| $f^{2/3}(a/r)^{4/3}v^{-1/3}$ | $r_i < r < D$ | swollen, three-dimensional | |
| $f^{2/3}(a/r)^{2/3}(a/D)^{2/3}v^{-1/3}$ | $D < r < fD$ | swollen, intermediate region | |
| $f^{2/3}(a/t)^{2/3}(a/D)^{2/3}v^{-1/3}$ | $fD < r < R_c$ | swollen, two-dimensional | |

Case II: $r_c \ll D \ll r_i$

| $\phi(r)$ | $r$ | region | |
|---|---|---|---|
| 1 | $0 < r < r_c$ | core | interior region |
| $f^{1/2}(a/r)$ | $r_c < r < D$ | ideal, three-dimensional | |
| $f^{1/2}(a/r)^{1/2}(a/D)^{1/2}$ | $D < r < fD$ | ideal, intermediate region | |
| $a/D$ | $fD < r < \tilde{r} \sim f(D/a)^{1/2}v^{-1/2}a$ | ideal, two-dimensional exterior region | |
| $f^{2/3}(a/r)^{2/3}(a/D)^{2/3}v^{-1/3}$ | $\tilde{r} < r < R_c$ | swollen, two-dimensional exterior region | |

structure of the free star is replaced by a five-zone scheme. The finer division is due to the appearance of an essentially two-dimensional region at the periphery of the star and of an intermediate region providing a smooth crossover to the three-dimensional interior. In the confined star as in the free star $\phi$ is a decreasing function of $r$. However, in the confined star $\phi$ decreases at a significantly lower rate. To complete this part of our discussion, we must find $R_c$, the radius of the confined star. To obtain $R_c$ we again use eq II.8. In the case $r_i \ll D \ll R$ we then have

$$Nfa^3 = \int_0^{R_c} \phi(r)\, d\mathbf{r} \sim \int_0^{r_c} r^2\, dr + f^{1/2}a\int_{r_c}^{r_i} r\, dr + f^{2/3}v^{-1/3}a^{4/3}\int_{r_i}^{D} r^{2/3}\, dr + f^{2/3}v^{-1/3}a^{4/3}D^{1/3}\int_D^{R_c} r^{1/3}\, dr \quad \text{(III.18)}$$

which yields

$$R_c \sim f^{1/4}v^{1/4}\left(\frac{D}{a}\right)^{-1/4}\left[N + \frac{1}{6}f^{1/2} + \frac{1}{10}f^{1/2}v^{-2} + \frac{3}{20}f^{-1/3}v^{-1/3}\left(\frac{D}{a}\right)^{5/3}\right]^{3/4} a \quad \text{(III.19)}$$

implicit to our case is the assumption that $N \gg f^{1/2}v^{-2}$; thus $R_c$ is given by

$$R_c \sim f^{1/4}v^{1/4}\left(\frac{a}{D}\right)^{1/4} N^{3/4}a \sim f^{-1/2}v^{1/4}\left(\frac{a}{D}\right)^{1/4} N_c^{3/4}a \quad \text{(III.20)}$$

where $N_c = fN$ is the total number of monomers in the star. $R_c$ is thus significantly smaller than $R_{cl}$, the radius of a confined linear chain, given by

$$R_{cl} \sim v^{1/4}\left(\frac{a}{D}\right)^{1/4} N_c^{3/4}a \quad \text{(III.21)}$$

When $r_c \ll D \ll r$. We distinguish between two possible situations: (1) $N \gg f^{1/2}v^{-2}$, i.e. "long-armed" stars with an extended swollen zone; (2) $f^{1/2}v^{-2} \gg N \gg f^{1/2}$, i.e., a "short-armed" star with an ideal "corona". For $N \gg f^{1/2}v^{-2}$, $R_c$ is given by

$$R_c \sim f^{1/4}\left(\frac{a}{D}\right)^{1/4} v^{1/4}\left[N + \frac{1}{6}f^{1/2} + \frac{1}{6}f^{-1/2}\left(\frac{D}{a}\right)^2 + \frac{1}{4}fv^{-1}\left(\frac{D}{a}\right) - \frac{1}{6}f\left(\frac{D}{a}\right)^2\right]^{3/4} a \quad \text{(III.22)}$$

which reduces, as expected, to (III.20). The radius of the "short-armed" star is given by

$$R_c \sim f^{1/2}\left[N + \frac{1}{6}f^{1/2} + \frac{1}{6}f^{-1/2}\left(\frac{D}{a}\right)^2 - \frac{1}{6}f\left(\frac{D}{a}\right)^2\right]^{1/2} a \quad \text{(III.23)}$$

Note that $R_c$ of the "short-armed" star is only weakly dependent on $D$.

## IV. Confinement Free Energy of a Single Star

Within the DC model it is natural to calculate the confinement free energy, $\Delta F_{con}$, by assigning $kT$ to each blob. $\Delta F_{con}$ is then given by

$$\frac{\Delta F_{con}}{kT} \sim \Delta N_b = N_{con} - N_{free} \quad \text{(IV.1)}$$

where $N_{con}$ and $N_{free}$ are the number of blobs in the confined star and in the free star. The use of this scheme is justified where blobs do not interpenetrate, i.e., in the swollen zone. Normally one hesitates to use this approach for ideal chains. However, the notion of ideal blobs in the star is related to the "temperature blob" model. In this model the chain is Gaussian on short chemical length scales but swollen on a larger scale. Furthermore, the blobs's structure of each of the star arms, including the ideal zone, is equivalent to that of a chain whose end group is grafted to the apex of a narrow cone with nonadsorbing walls. It is, then, justified to use this scheme for both the ideal and the swollen zone if we take care to count only the *smallest nonoverlapping* blobs: in the swollen part of the exterior region one counts $D$ blobs while in the ideal part only superblobs should be counted. The use of (IV.1) in the case $r_i \ll D \ll R$ where this issue does not arise is certainly justified.

To calculate $\Delta N_b$ we use an argument due to Witten and Pincus[10] which enables us to calculate the number of blobs in the *self-similar* regions of the star. The resulting $\Delta F_{con}$ is valid when the non-self-similar intermediate region is comparatively small, i.e., when $D \ll R$. In a self-similar region, the blobs in a certain shell are $\omega$ times larger than the blobs in the adjacent inner shell. As a result, the thickness of the region is given by a geometrical progression. Thus, on knowing the boundaries of the region we may obtain the number of shells in it. For any shell, $j$, in a self-similar region we have

$$\frac{\xi_{j+1}}{\xi_j} = \frac{r_{j+1}}{r_j} \simeq 1 + \frac{\xi_j}{r_j} \equiv \omega \quad \text{(IV.2)}$$

Comparing (IV.2), (III.2), and (II.1), we find

$$\omega = 1 + f^{-1/2} \quad \text{interior region} \quad \text{(IV.3a)}$$

$$\omega = 1 + f^{-1} \quad \text{exterior region} \quad \text{(IV.3b)}$$

The number of shells $S$ in a region is thus given by

$$r_u - r_l \sim \xi(r_l)(1 + \omega + \ldots + \omega^{s-1}) = \xi(r_l)\frac{\omega^s - 1}{\omega - 1} \quad \text{(IV.4)}$$

where $r_u$ and $r_l$ are the upper and lower radii of the said region. We then find

$$S \sim \frac{\ln (r_u/r_l)}{\ln \omega} \sim f^{1/2} \ln (r_u/r_l) \qquad \text{interior region} \tag{IV.5a}$$

$$\sim f \ln (r_u/r_l) \qquad \text{exterior region} \tag{IV.5b}$$

The structure of a free star is that of the interior region. All relevant zones are self-similar and there are $f$ blobs per shell. The number of blobs in the ideal zone of the free star is then

$$N_i = fS_i \sim -f^{3/2} \ln \upsilon \tag{IV.6}$$

Tne number of blobs in the swollen zone is given by

$$N_s = fS_s \sim f^{3/2} \ln (N\upsilon^{-2}f^{-1/2}) \tag{IV.7}$$

One must exercise care in applying this method to confined stars. In the swollen zone of the exterior region we must count $D$ blobs whose number is not given by $fS$. Furthermore, the Witten–Pincus method is not easily applied to the intermediate region, which is not self-similar. Let us first consider the case $r_i \ll D \ll R$. There are three zones which are relevant to the calculation of $\Delta F_{con}$: (1) $r_i < r < D$, the swollen zone of the interior region (In this zone there are $f$ blobs per shell. The size of the blob is $\xi \sim f^{-1/2}r$); (2) $D < r < fD$, the intermediate region (Again we have $f$ blobs per shell. This region is not self-similar and $\xi \sim f^{-1/2}r^{1/2}D^{1/2}$); (3) $fD < r < R_c$, the exterior region, which is swollen in this case (Here there are $n_b \sim f^{-4/3}r^{4/3}D^{-4/3}$ $D$ blobs per shell. $\xi \sim f^{-1}r$). We will denote the number of shells and of blobs in the $i$'s zone by $S_i$ and $N_i$, respectively. Using IV.5, we find

$$N_1 = fS_1 \sim f^{3/2} \ln (\upsilon(D/a)f^{-1/2}) \tag{IV.8}$$

Since the intermediate region is not self-similar, $\omega$ is a function of $r$. To obtain an estimate of $N_2$ we use an average $\omega$, $\langle\omega\rangle$, given by

$$\langle\omega\rangle \simeq \frac{\int_D^{fD} \omega(r)\, dr}{fD - D} \sim \frac{1}{fD}\int_D^{fD} (1 + \tfrac{1}{2}f^{-1/2}D^{1/2}r^{-1/2})\, dr \sim 1 + 1/f \tag{IV.9}$$

In the intermediate region $\langle\omega\rangle$ is identical with $\omega$ of the exterior region. Using IV.4 and approximating $fD - D \simeq fD$, we find $S_2 \sim f^{3/2}$ and

$$N_2 = fS_2 \sim f^{5/2} \tag{IV.10}$$

The number of shells in the exterior region is given by

$$S_3 \sim f \ln [f^{-3/4}(a/D)^{5/4}\upsilon^{1/4}N^{3/4}] \tag{IV.11}$$

In this region $N_3 \neq fS_3$; rather, we have

$$N_3/f \sim n_b(fD)(1 + \omega^{4/3} + ... + \omega^{4S_3/3-1}) \sim \tfrac{3}{4}f(\omega^{4S_3/3} - 1) \tag{IV.12}$$

giving

$$N_3 \sim f(a/D)^{5/3}\upsilon^{1/3}N \tag{IV.13}$$

We find that $\Delta N_b$ for the case $r_i \ll D \ll R$ is given by

$$\Delta N_b = N_1 + N_2 + N_3 - N_s \tag{IV.14}$$

giving

$$\frac{\Delta F_{con}}{kT} \sim f^{3/2} \ln \left(\upsilon\frac{D}{a}f^{-1/2}\right) + f^{5/2} + f\left(\frac{a}{D}\right)^{5/3}\upsilon^{1/3}N - f^{3/2} \ln (N\upsilon^{-2}f^{-1/2}) \tag{IV.15}$$

For $N \gg f^{1/2}\upsilon^{-2}$ and $D \ll R$, we have

$$\frac{\Delta F_{con}}{kT} \sim fN\upsilon^{1/3}(a/D)^{5/3} \sim N_c\upsilon^{1/3}(a/D)^{5/3} \tag{IV.16}$$

where $N_c = fN$. Note that $\Delta f_{con}$ is identical with that of a linear chain consisting of $N_c$ monomers.[3a]

In the case $r_c \ll D \ll r_i$ we must distinguish between two possibilities: (1) $N \gg f^{1/2}\upsilon^{-2}$ (in this case the confined star has an extended swollen exterior region); (2) $f^{1/2}\upsilon^{-2} \gg N \gg f^{1/2}$ (the exterior region contains an ideal zone only). Let us begin with the first situation, of "long-armed" stars. To obtain $\Delta N_b$ we need to know the number of blobs in four zones: (1) $r_c < r < D$, the idel interior zone. In it, each shell contains $f$ blobs of size $\xi \sim f^{-1/2}r$. (2) $D < r < fD$, the intermediate zone. Here there are $f$ blobs of size $\xi \sim f^{-1/2}r^{1/2}D^{1/2}$ in each shell. (3) $fD < r < f(D/a)^{1/2}\upsilon^{-1/2}a$, the ideal exterior zone. Each shell consists of $f$ superblobs of size $\xi \sim f^{-1}r$. (4) $f(D/a)^{1/2}\upsilon^{-1/2}a < r < R_c$, the swollen exterior zone. Each shell contains $n_b \sim f^{-4/3}r^{4/3}D^{-4/3}$ $D$ blobs. $\xi \sim f^{-1}r$. Using IV.4, we find

$$N_1 \sim fS_1 \sim f^{3/2} \ln (f^{-1/2}D/a) \tag{IV.17}$$

The number of blobs in the intermediate region is given by (IV.10). By using eq IV.4 we obtain

$$N_3 \sim fS_3 \sim f^2 \ln [(D/a)^{1/2}\upsilon^{-1/2}] \tag{IV.18}$$

To obtain the number of $D$ blobs in the swollen exterior zone we use the same procedure as before, taking into account the shift in the boundaries. $N_4$ is given by (IV.13). $\Delta F_{con}$ is thus given by

$$\Delta F_{con}/kT \sim N_1 + N_2 + N_3 + N_4 - N_i - N_s \sim f^{3/2} \ln \left(f^{-1/2}\frac{D}{a}\right) + f^{5/2} + f^2 \ln \left[\left(\frac{a}{D}\right)^{1/2}\upsilon^{-1/2}\right] + f\left(\frac{a}{D}\right)^{5/3}\upsilon^{1/3}N + f^{3/2} \ln \upsilon - f^{3/2} \ln (N\upsilon^{-2}f^{-1/2}) \tag{IV.19}$$

For $N \gg f^{1/2}\upsilon^{-2}$ and $D \ll R$, $\Delta F_{con}$ is given as before by (IV.16). For "short-armed" stars ($f^{1/2}\upsilon^{-2} \gg N \gg f^{1/2}$), $N_4 = 0$ and the dominant term is $N_3$, leading to

$$\frac{\Delta F_{con}}{kT} \sim f^2 \ln \left(f^{-1}\frac{Na^2}{D^2}\right) \tag{IV.20}$$

In this case $\Delta F_{con}$ is only weakly dependent on $D$.

## V. Concentration Effects

Single-star effects control the behavior of dilute solutions of stars in a slit. When the concentration is increased past a critical overlap concentration, $C_1$, the fringes of different stars begin to interpenetrate. The overlap regions locally resemble a semidilute solution of linear chains. In this regime screening competes with confinement. The effect of screening grows with the concentration: the screening length, the size of the concentration blob, decreases with increased concentration. Thus, when the concentration is increased, the two-dimensional behavior caused by the confinement is smeared out. The picture that emerges is similar to that of linear chains confined to a slit as analyzed by Daoud and de Gennes (DdG).[3a] Following DdG we display the various regimes of a solution of "long-armed" ($N \gg f^{1/2}\upsilon^{-2}$) stars in a slit on a diagram with axes $x$ and $y$ (Figure 2) defined by

$$y = R/\xi(C) \sim (C/C^*)^{3/4}; \qquad x = R/D \tag{V.1}$$

In terms of $x$, $R_c$ may be written as

$$R_c \sim Rx^{1/4} \tag{V.2}$$

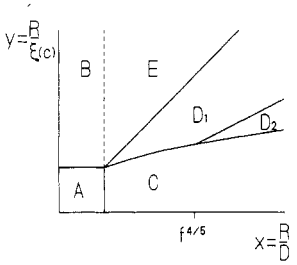


**Figure 2.** Various regimes of solutions of star polymers in a slit. For linear chains, there is no distinction between regions $D_1$ and $D_2$.

The critical overlap concentration in a slit is now a function of $x$; specifically

$$C_1 = \frac{Nf}{R_c^2 D} \sim f^{1/2}N^{-1/2}v^{-1/2}a^{-3}\left(\frac{a}{D}\right)^{1/2} \sim C^*x^{1/2} \qquad D < R \tag{V.3a}$$

$$C_1 = \frac{Nf}{R^3} = C^* \qquad D > R \tag{V.3b}$$

$C_1$, in terms of $C^*$ and $x$, has the same form as that of confined linear chains. For $x \geq 1$ and $y \leq 1$ (region A) we have a dilute solution of spherical stars. When $D$ decreases, the stars are deformed into pancakes. For $x \leq 1$ the region below the curve

$$y \sim x^{3/8} \tag{V.4}$$

(region C) corresponds to a dilute solution of "pancakes"—confined stars. For weak confinement, i.e., $R \leq R_c \leq fD$ or $1 \leq x \leq f^{4/5}$, the confined star has no exterior region. In this regime, the sole result of the confinement is the appearance of an intermediate region. Starting from region C, of dilute noninteracting pancakes, we now increase the concentration so as to force separate pancakes to overlap; i.e., we increase $y$ past the $y \sim x^{3/8}$ boundary. To account for overlap effects we introduce a crossover distance $\chi_c(C)$, similar to $\chi(C)$ defined by (II.11) for free stars. For $r < \chi_c(C)$ we find single-star behavior while for $r > \chi_c(C)$ we find concentration blobs of single size. To obtain $r < \chi_c(C)$ we equate $\phi(\chi_c)$ with the "bulk" monomer volume fraction $Ca^3$; we find

$$\chi_c \sim fv^{-1/2}(Ca^3)^{-3/2}\frac{a}{D}a \sim R_c\left(\frac{C_1}{C}\right)^{3/2} \sim Rxy^{-2} \tag{V.5}$$

In terms of $\chi_c$ we may distinguish two regimes: (1) $R_c > \chi_c > fD$, "semidilute solution of two-dimensional confined stars" (regime $D_1$). In this regime each star has an exterior region characterized by a two-dimensional behavior. This regime is obtained for $C_1 < C < C_2$, where

$$C_2 \sim C^*f^{-2/3}x^{4/3} \sim (a/D)^{4/3}a^{-3}v^{-1/3} \tag{V.6}$$

The upper boundary of this regime is given by

$$y \sim f^{-1/2}x \tag{V.7}$$

The upper and lower boundaries of $D_1$ intersect at $x = f^{4/5}$, $y = f^{3/10}$. (2) $fD > \chi_c > D$, "semidilure solution of three-dimensional confined stars" (regime $D_2$). In this regime the exterior region structure is lost, for any $x$, because of the screening. The main effect of the confinement is in the existence of the intermediate region. This regime is found for $C_2 < C < C_3$, where

$$C_3 \sim C^*x^{4/3} \tag{V.8}$$

The upper boundary of this regime is thus given by

$$y \sim x \tag{V.9}$$

$D_1$ and $D_2$ replace a single regime, $D_0$, found for confined linear chains.[3a] For $y < x$ we cross into region E, in which all correlation lengths are smaller than the slit thickness $D$. This region is essentially indistinguishable from region B of semidilute stars (bounded by $x = y = 1$).

In regions A[10] and C, where different stars do not overlap, we expect the osmotic pressure to obey the ideal gas law

$$\Pi/kT \sim C/Nf \tag{V.10}$$

When different stars interpenetrate to a significant degree, as in regions B,[10] E, $D_1$, and $D_2$, we expect the osmotic pressure of a semidilute solution of linear chains

$$\Pi/kT \sim (1/a^3)(Ca^3)^{9/4} \tag{V.11}$$

The confinement free energy, $\Delta F_{con}$, in regions $D_1$ and $D_2$ is different. In $D_1$ $\Delta F_{con}$ is significantly larger because of the contribution of the exterior region, which is screened out in region $D_2$. As a result, stars in regions $D_1$ and $D_2$ differ in their chemical potentials, while their osmotic pressures are very similar.

## VI. Discussion

A free star is characterized by its spherical symmetry. For confined stars, this picture changes into a three-region scheme: (1) an interior region, unaffected by the confinement, which retains its original spherical symmetry; (2) an intermediate, non-self-similar region, in which the spherical symmetry is lost because of the confinement, but blobs are still three-dimensional; (3) an exterior region characterized by its cylindrical symmetry. In this region, the three-dimensional blobs are replaced by two-dimensional superblobs, composed of blobs of size $D$. This three region structure is a special feature of confined star polymers.

This type of analysis is best suited for the case of long-armed stars ($N \gg f^{1/2}v^{-2}$) under strong confinements, such that only the swollen zone is affected ($r_i \ll D \ll R$). For such a case, one need not worry about spurious effects due to the structure of the center, or the validity of scaling concepts for short-chain segments. Furthermore, this case corresponds to that of a colloidal particle coated by densely grafted chains. In this case the following conclusions hold: (1) The concentration profile of the periphery of the star decays as $r^{-2/3}$, compared with $r^{-4/3}$ for the free star. (2) The radius of the star in the slit plane is $f^{-1/2}$ times smaller than that of a linear chain with an equal number of monomers. (3) The confinement free energy of a star is identical with that of an equivalent linear chain.

Mica plate experiments[11] seem to offer the best hope for a direct experimental test of our results. The force law observed between coated plates is directly related to the confinement free energy. In our case, the force law between a bare plate and a plate coated by nonoverlapping grafted star polymers should provide the desired data.

**Acknowledgment.** The Fritz Haber Research Center is supported by the Minerva Gesellschaft für die Forschung, mbH, München, BRD.

## References and Notes

(1) Cotton, C. K.; Statterfield, C. M.; Lai, C. J. *AIChE J.* **1975**, *21*, 289.
(2) (a) Halperin, A.; Pincus, P.; Alexander, S. *J. Phys., Lett.* **1985**, *46*, 2543. (b) Halperin, A.; de Gennes, P.-G. *J. Phys. (Les Ulis, Fr.)* **1986**, *47*, 1243. (c) Boudoussier, M., to be published.
(3) (a) Daoud, M.; de Gennes, P.-G. *J. Phys. (Les Ulis, Fr.)* **1976**, *38*, 85. (b) de Gennes, P.-G. *Scaling Concepts in Polymer Physics*; Cornell University: Ithaca, NY, 1979. (c) Turban, L. *J. Phys. (Les Ulis, Fr.)* **1984**, *45*, 347.
(4) (a) Lubensky, T. C.; Issacson, J. *J. Phys. (Les Ulis, Fr.)* **1981**, *42*, 175. (b) Gaunt, D. S.; Lipson, J. E. G.; Martin, J. L.; Sykes, M. F.; Torrie, G. M.; Whittington, S. G.; Wilkinson, M. K. *J.*

Phys. A: Math. Gen. 1984, 17, 211.
(5) Daoud, M.; Cotton, J. P. J. Phys. (Les Ulis, Fr.) 1982, 43, 531.
(6) Birshtein, T. M.; Zhulina, E. B. Polymer 1984, 25, 1453.
(7) Huber, K.; Burchard, W.; Fetters, L. J. Macromolecules 1984, 17, 541.
(8) Miyake, A.; Freed, K. F. Macromolecules 1983, 16, 1228.
(9) (a) Weil, G.; des Cloizeaux, J. J. Phys. (Les Ulis, Fr.) 1979, 40, 99. (b) Akcasu, A.; Han, C. C. Macromolecules 1979, 12, 276.
(10) Witten, T.; Pincus, P. Macromolecules 1986, 19, 2509.
(11) (a) Klein, J. Nature (London) 1980, 288, 248. (b) Hadziioannou, G.; Patel, S.; Granick, S.; Tirrel, M. J. Am. Chem. Soc., in press.

# Least-Draining Limit of Linear Flexible Chain Molecules

**J. J. H. Mulderije and H. L. Jalink***

*Department of Physical and Macromolecular Chemistry, Gorlaeus Laboratories, University of Leiden, 2300 RA Leiden, The Netherlands.* *Received May 9, 1986*

ABSTRACT: A theoretical study has been made to decide whether in the so-called non-free-draining limit of a linear flexible chain without excluded volume the inner region of the chain domain is asymptotically nondrained. To this end the average velocity perturbation field of the solvent medium resulting from a single chain in uniform translation, and observed from the center of mass, is calculated with the bead–string model of Kirkwood and Riseman. Only the asymptotic limit for a large number of segments is considered. In the approximation obtained, the average fluid velocity relative to the stationary molecule and at the center of mass is 3.6% of the unperturbed velocity whereas at a radial distance beyond which on the average half of the segments is present the relative velocity in the equatorial plane is 36% of the unperturbed velocity. Average perturbation fields have also been calculated as observed from the middle and end segments of the chain. These fields are markedly different. It is concluded that words like "the nondraining limit" and "the impermeable limit", which long have been widely used, refer to a hydrodynamical condition that for unbranched flexible polymers is never obtained. We suggest the use of terms like "the least-draining limit" or "limit of smallest drain".

## Introduction

Ever since its introduction by Kirkwood and Riseman[1] (KR) in 1948, the spaced bead–string model in conjunction with the Oseen hydrodynamic interaction between the beads has appeared in theories on the intrinsic viscosity $[\eta]$ and the friction coefficient $f$ of dilute polymer solutions.[2] In this model two limiting states are discerned, the "free-draining limit", and its opposite, the "non-free-draining case", cautiously named so by Yamakawa in his monograph.[2] The latter limit is all-important because the behavior of real polymer solutions usually conforms to this limit.

The term "non-free-draining" leaves open the question whether the solvent in the interior of the chain domain is immobilized with respect to the chain. Over many years, however, terms like "the nondraining limit" and "the impermeable limit" have been in vogue.[3] The idea of a chain molecule being nondrained for high degrees of polymerization was suggested by the results obtained by Debye and Bueche[4] in their calculation of $[\eta]$ and $f$ using a sphere of uniform segment density. They introduced the concept of hydrodynamical shielding and the "shielding length" $L$ ($L = [\eta_0/\nu\zeta]^{1/2}$, $\nu$ is the bead density and $\zeta$ is the friction coefficient of a bead).[5] For large values of the "shielding ratio" $\sigma$ ($=R_s/L$, with $R_s$ the radius of the sphere), $[\eta]$ and $f$ approach values that hold for impermeable spheres of radius $R_s$. Apparently, there is exclusion of flow lines from the interior of the sphere in these cases.

It is a well-known result of the KR theory for the bead string model that for large values of $nr_b/R_g$ ($r_b = \zeta/6\pi\eta_0$ is the bead radius, $n$ is the total number of beads, and $R_g$ is the radius of gyration of the chain), $[\eta]$ and $f$ become independent of $\zeta$. Besides, the average drift velocities of the beads vanish $\sim n^{-1/2}$ ($\Theta$ state). From these results, Kirkwood and Riseman concluded that the interior segments of a long flexible chain are likewise hydrodynamically shielded.

Evaluation of the shielding ratio for the chain will only fortify this opinion. Making use of the spherically symmetric Gaussian approximation for the segment distribution[2]

$$\nu(r) = n\left(\frac{3}{2\pi R_g^2}\right)^{3/2} \exp\left(-\frac{3r^2}{2R_g^2}\right) \qquad (1)$$

in which $R_g^2 = nb^2/6$, $b$ being the distance between the segment beads, we consider the succession of shells of varying segment density. Thus we obtain

$$\sigma_{ch} = \int_0^\infty \frac{dr'}{L(r')} = \left(\frac{\zeta}{\eta_0}\right)^{1/2} \int_0^\infty \{\nu(r')\}^{1/2}\, dr' = \left(\frac{3\zeta}{2b\eta_0}\right)^{1/2}\left(\frac{n}{\pi}\right)^{1/4} \qquad (2)$$

It is seen that $\sigma_{ch}$ increases with $n^{1/4}$, as it does for a sphere of uniform segment density.

Flory[6] was very definite in the matter, writing "once $\zeta/\eta_0$ is great enough to exclude the flow lines from the interior region of the molecule". These words suggest that $\zeta/\eta_0$ might be raised at will independent of the bead density. This cannot be true, however. Accordingly as the real chain bears more side groups, it becomes stiffer. Consequently we have to assume a greater value for the bead–bead distance of the equivalent statistical chain, which has free rotation of segments. As one bead has to represent a larger section of the chain, the size of the beads increases and their number decreases. In this way, while $\zeta/b$ is slowly varying, the value of the well-known draining parameter $h$ (eq 27) will decrease through the factor $n^{1/2}$, rather than increase.

Whatever the thickness of the real chain, when the chain statistics is Gaussian or not very different, the segment density in a point defined with respect to the center of

0024-9297/87/2220-1152$01.50/0 